Brillouin-light-scattering study of long-wavelength spin waves in a single-crystal 300-Å gadolinium film

S. H. Kong, M. V. Klein, F. Tsui, and C. P. Flynn
Department of Physics, University of Illinois at Urbana-Champaign, 1110 West Green Street, Urbana, Illinois 61801
(Received 7 October 1991; revised manuscript received 26 December 1991)

The temperature dependence of the energy of ferromagnetic spin waves in an epitaxially grown 300-Å [0001] Gd film is shown to depend on the bulk values of the c-axis magnetic-stiffness constant D_c, defined by $\omega(\mathbf{q})=\sum_i D_i q_i^2$, where $|qa|\ll 1$, and the axial-anisotropy constant P_2, defined by $\mathcal{H}_{\text{aniso}}=P_2(S_z)^2+\cdots$. Two bulk spin waves and one Damon-Eshbach surface magnetostatic wave were probed with Brillouin light scattering. The bulk spin waves were found to be sensitive to the exchange interaction. In contrast, the Damon-Eshbach surface magnetostatic wave, although insensitive to the exchange interaction, is influenced noticeably by the axial magnetic anisotropy $P_2(T)$ present in Gd. Ignoring surface anisotropy, we extracted values of $D_c(T)$ and $P_2(T)$ from the Brillouin data and from the magnetization of the Gd film determined by a superconducting-quantum-interference-device magnetometer. Within the experimental errors, these values are reasonably consistent with the bulk values from the literature.

I. INTRODUCTION

The bulk magnetic properties of the heavy rare-earth (HRE) metals were investigated extensively in the 1960s and 1970s,[1] highlighted by the study of their various magnetic structures and of spin waves through neutron-scattering techniques. Recently, neutron-scattering studies have also been instrumental in the determination of the magnetic structure of molecular-beam-epitaxy (MBE) -grown single-crystal HRE superlattices.[2–4] However, very few light-scattering experiments on HRE metals have been documented. Recently, in a collaborative effort to explore the behavior of HRE films, we initiated a Raman light-scattering study of MBE-grown single-crystal Dy, Er, and Y films.[5] The transverse-optical phonons and electronic excitations in Dy, Er, and Y films, and the acoustic ferromagnetic spin wave in Dy films were investigated.

Some of the early Brillouin-light-scattering studies on opaque ferromagnets were performed on EuO, as well as Fe and Ni.[6,7] In the present paper, we report a Brillouin study on a HRE film. Three acoustic spin were observed in an epitaxially grown 300-Å [0001] Gd film. The spin-wave frequencies were tracked as a function of temperature and wave vector. Gd was chosen for this Brillouin study, since it is a ferromagnet with small magnetic anisotropy, unlike the other HRE metals, which posses magnetic phases with oscillatory spin structures and large anisotropy. A good foundation already exists for understanding the Brillouin spectra of spin waves in opaque ferromagnets such as Fe, and we use this machinery to analyze the data from Gd. The analysis shows that the dispersion of the bulk modes is sensitive to the exchange interaction, and the c-axis magnetic-stiffness constant $D_c(T)$ has a value and temperature dependence consistent with that extracted from neutron data. We also find it necessary to include the lowest-order axial anisotropy.

Gadolinium. Six of the heavy rare-earth metals order magnetically: Gd, Tb, Dy, Ho, Er, Tm. The systematically varying $4f$ shells distinguish their magnetic behaviors from one another. Gd does not have the nearly two-dimensional nesting feature in its hole Fermi surface.[1] It therefore is the only element out of the six that does not posses at least one helimagnetic phase. Gd is a ferromagnet below its Curie temperature of 293 K. It has a half filled $4f$ shell; hence, $L=0$ and $S=7/2$. Since Gd is an S-state ion, the magnetic anisotropy is relatively weak; however, it still plays a major role in the unusual temperature dependence of the easy axis direction. Above 248 K, the easy axis is along the c axis. Below that temperature the moments tilt away from the c-axis, with a maximum tilt of 75° at 195 K, and approach 32° at low temperatures.[8] There is no apparent easy direction in the basal plane. During the measurements made on the 300-Å Gd film, the moments are forced to lie in the plane of the film by the demagnetization factor and the applied magnetic field.

II. EXPERIMENTAL TECHNIQUES

A. Sample growth

The 300-Å single-crystal Gd sample was grown in a Perkin Elmer 400-MBE chamber, using growth procedures similar to those of Ref. 9. At a pressure on the order of 10^{-10} Torr, 500 Å of [110] Ta was first grown on a $4.0\times4.0\times0.6$ mm^3 [11$\bar{2}$0] sapphire substrate at 900 °C for chemical separation. A 2800-Å [0001] Y buffer was then deposited at 500 °C. The [0001] Gd film was grown at 400 °C with a growth rate of approximately 0.5 Å/sec. *In situ* structural characterization by reflection high-energy electron diffraction indicated that the sample has an atomically flat surface with in-plane coherence length

greater than 100 Å. The deposition rate was monitored *in situ*, by a quartz-crystal monitor, and the frequency shift of the quartz crystal was recorded and calibrated by a linear profilometer. A 6000-Å Gd film was grown simultaneously with the 300-Å film, and its thickness was measured by a linear profilometer to within 200 Å. From this calibration of the thicker film, we obtained the thickness of the 300-Å Gd film with an uncertainty of approximately 5–10 %. The sample was stored in an evacuated desiccator jar and exposed to air only upon transfer to the cryostat.

B. Magnetization measurements

The magnetization of the Gd film must be known in order to calculate the spin-wave frequencies using the dipole-exchange dispersion relations. The temperature dependence of the in-plane field-cooled magnetization of the Gd film of the sample was measured with a Quantum Design superconducting-quantum-interference-device (SQUID) magnetometer. In the Brillouin experiments, fields of 1.0 and 4.8 kOe were applied in the plane of the film and parallel to the edge of the sapphire substrate. Laue x-ray scattering on the substrate determined that this edge approximately bisects the a and b axes of the Gd film. In the SQUID measurements, fields of 1.06 and 4.6 kOe were applied in the same orientation.

The diamagnetic contribution of the sapphire substrate and the sample holder is nearly temperature independent. It was subtracted using a linear fit to the $T = 100$-K field dependence of the magnetization above saturation and extrapolating to zero field. The diamagnetic contribution to the total moment of the sample is on the order of 2.9×10^{-5} and 1.4×10^{-4} emu for a 1.0 and 4.8 kOe applied fields, respectively. The small paramagnetic contribution by the conduction electrons in the tantalum and yttrium layers is also included in these figures. This weakly temperature-dependent contribution is on the order of 10^{-7} emu. The temperature dependence introduces uncertainty on the order of 10^{-8} emu, which is negligible compared to the total moment of the sample, which is on the order of 2×10^{-3} emu.

The measured moment of the sample was used in conjunction with the measured volume to calculate the magnetization. Taking into account the uncertainties in the thickness and the film dimensions, the uncertainty in the volume estimates were on the order of 5–10 %. A constant uncertainty in the magnetization was also introduced when the diamagnetic contribution was estimated and subtracted. This was on the order of 1% of the total moment. In agreement with these estimates, the low-temperature magnetization was found to approach a value near to the known full saturation value of 2118 G.

The magnetization results are shown in Fig. 1. The small softening in the ($H = 1.0$ kOe) magnetization curve at low temperatures is due to moments tilting out of the plane of the film as a consequence of the magnetic anisotropy. The magnetization data for bulk Gd were determined by neutron scattering[8] and corresponds to the case of zero applied magnetic field. The small discrepancies between the magnetization curves of the film and the bulk Gd may be attributed to the overestimation of the film volume or the moments at the Gd/Y interface if they are not fully saturated.

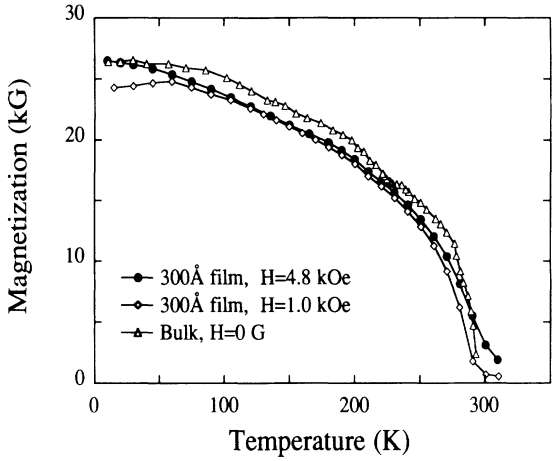

FIG. 1. The magnetization curves of the 300-Å Gd film measured with a SQUID magnetometer with the magnetic field **H** applied in the plane of the film and 15° from the a axis. They are compared with the b-axis magnetization curve for bulk Gd determined by neutron scattering (Ref. 8).

C. Brillouin scattering

Inelastic light scattering, such as Brillouin scattering, probes long-wavelength excitations near the Brillouin-zone center. The wavelength of visible light is on the order of 600 nm, and the wave vector is on the order of 10^6 cm^{-1}. For light probing excitations traveling parallel to the surface, the maximum wave vector accessible is on the order of 2×10^6 cm^{-1}, which corresponds to wavelengths on the order of 300 nm. As the excitation wavelength is much smaller than the lateral dimensions of the sample, traveling waves are probed and edge effects can be ignored.

The penetration depth of light in Gd is 200 Å. Since light only penetrates a small distance into a metal, the conservation rule for the normal component of wave vector is relaxed; therefore, only the parallel components of the wave vectors of the incident and scattered light are relevant to consider in the momentum selection rules. As a result, the spectrum of bulk modes is broad, since light is scattered from a continuum of modes. In thin films, the spin waves travel parallel to the surface, so that wave vector in this case is strictly conserved and discrete bulk modes are observed. The dispersion of these modes may be studied by varying the backscattering angle. A review of light scattering from opaque ferromagnetic films can be found in Ref. 10 and a rigorous treatment found in Ref. 11.

A Sandercock tandem Fabry-Perot interferometer was used in the six-pass configuration for the Brillouin experiments. The 6471-Å line of a Coherent krypton-ion laser providing a single-moded power of 100–150 mW was the light source for all of the scans. The experimental setup is diagramed in Fig. 2. True backscattering was achieved

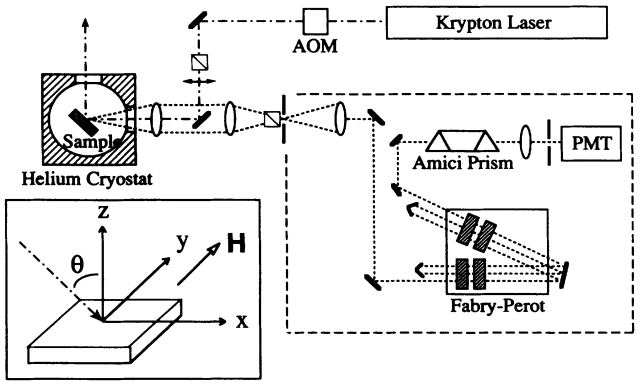

FIG. 2. The experimental setup for the Brillouin experiment; two pinhole lens combinations act as spatial filters, and one combination of Amici prism-pinhole lens acts as a band pass filter. A cube polarizer sits before the pickoff mirror in order to select the p polarization for the incident beam. The analyzing polarizer sits in front of the first pinhole. The inset shows the scattering geometry.

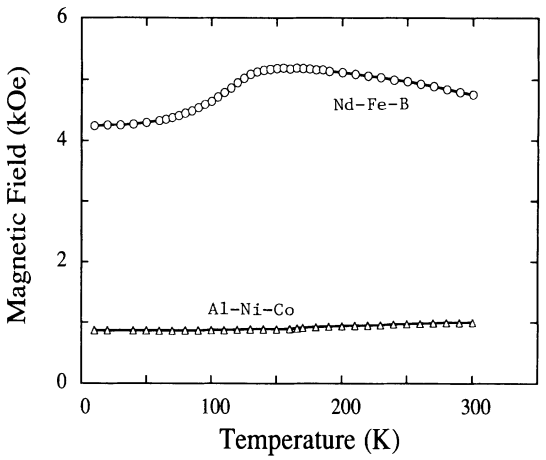

FIG. 3. The temperature dependence of the magnetic field at the center of the gap of two sets of permanent magnets used in the Brillouin experiments: (○) Nd-Fe-B and (△) Al-Ni-Co.

by using a pickoff mirror in front of the focusing and/or collecting lens. The angle between the incident ray and the sample normal will be defined as the "backscattering angle." An acoustic-optic modular attenuates the beam when scanning through the laser line.

The sample was cooled by a He cryostat and mounted on a solid brass finger that extends from the probe. The base of this finger is cylindrical. A temperature diode is mounted into the base, and the heater wire is wound around the base. A magnetic field was applied by various sets of permanent magnets attached to a soft iron yoke. The gap provided by the yoke was 6.4-mm wide with cross sectional dimensions of 12.7×7.9 mm.^{2} Al-Ni-Co magnets were used to generate a 1.0-kOe field and Nd-Fe-B magnets to generate a 4.8-kOe field, at room temperature. The fields of the magnets are temperature dependent, and they have been calibrated using a Hall probe. The calibration curves for the magnetic field in the gap of the permanent magnet systems are shown in Fig. 3. Note the rather large temperature dependence of the Nd-Fe-B magnets.

The incident polarization of light was selected to be in the plane of reflection for optimal penetration into the metal surface. The analyzer may be removed in order to obtain the unpolarized spectrum or inserted to obtain the polarized $z(xx)\bar{z}$ or depolarized $z(xy)\bar{z}$ spectrum. In the backscattering geometry, spin waves scatter light mainly in the depolarized configuration, while elastic waves scatter light in the polarized configuration. As a result, elastic waves and spin wave may be distinguished from one another by examining the polarized and depolarized spectra. From the scatter in the Brillouin data, it is estimated that the relative uncertainty in the extracted peak positions is at most 0.5 GHz. Most of the uncertainties result from determining the spectral calibration. However, the accuracy of the temperature readings may cause an additional systematic error in the temperature dependence of the peak positions. This accuracy is limited by the calibration of the temperature diode and the effect of local heating of the sample by the laser light.

The local sample temperature of the region probed is elevated by a few degrees kelvin by the incident laser power. By varying the laser power from 20 to 300 mW and tracking the shallow surface mode frequency, it was determined that the incident power of 150 mW used during the scans raised the local temperature by approximately 4 K when the temperature was set to 250 K. A detailed and time consuming calibration at all temperatures has not been done and is not necessary until a detailed study on the critical behavior of the magnetic-stiffness constant is initiated. Since it is not reasonable to assume that the local temperature is raised by 4 K for all temperature settings, the temperature dependence is left uncalibrated.

III. SPIN WAVES

A. Bulk spin waves in ferromagnetic films

Spin waves are quantized excitations of the transverse component of the magnetization. Near the region of the Brillouin-zone center accessible by visible light scattering, the dominant interaction that determines the acoustic spin-wave frequencies in bulk Gd is the dipole-dipole interaction. The magnetic anisotropy is very small so the large acoustic spin-wave gap energy of about 22 cm^{-1} observed in the Dy is absent in Gd. If we neglect the exchange interaction, the long-wavelength bulk spin waves are dispersionless, and the medium may be treated as a magnetic continuum. It is more proper to call these modes magnetostatic waves instead of spin waves, since spin waves technically refers to waves dominated by the exchange interaction. However, for simplicity we may also refer to them as spin waves. The inclusion of the exchange interaction results in a q^2 dispersion. This contri-

bution to the frequency is relatively small in the region probed, but this term is important in thinner films where standing waves are present perpendicular to the film with wavelengths that are much shorter than the propagation wavelength. Before considering this case, we first examine the dispersion of spin waves in thick Gd films.

The Hamiltonian relevant for acoustic magnons in an hcp ferromagnet is given by

$$\begin{aligned}
&\mathcal{H}=\mathcal{H}_{\text{dipole}}+\mathcal{H}_{\text{Zeeman}}+\mathcal{H}_{\text{aniso}}+\mathcal{H}_{\text{exch}}\ ,\\
&\mathcal{H}_{\text{dipole}}=\sum_{n>m}\frac{g^2\mu_B^2}{r_{\text{nm}}^3}\left[\mathbf{S}_n\cdot\mathbf{S}_m-\frac{3}{r_{\text{nm}}^2}(\mathbf{S}_n\cdot\mathbf{r}_{\text{nm}})(\mathbf{S}_n\cdot\mathbf{r}_{\text{nm}})\right]\ ,\\
&\mathcal{H}_{\text{Zeeman}}=-g\mu_B H\sum_n S_n^{\zeta}\ ,\\
&\mathcal{H}_{\text{aniso}}=\sum_n\{P_2(S_n^z)^2+P_4(S_n^z)^4+P_6(S_n^z)^6+P_6^6[(S_n^+)^6+(S_n^-)^6]\}\ ,\\
&\mathcal{H}_{\text{exch}}=-\sum_{n\neq m}J(\mathbf{r}_{\text{nm}})\mathbf{S}_n\cdot\mathbf{S}_m\ .
\end{aligned}\tag{1}$$

The x, y, and z axes correspond to the a, b, and c axes of the hcp crystal. The ζ axis is defined to be along the direction of the applied magnetic field. In this paper the ζ axis will be confined to the basal plane. J is the exchange function. S_n and S_m are the total angular momentum of the ions localized at r_n and r_m; P_2, P_4, P_6 are the axial, and P_6^6 the planar anisotropy constants for Gd. P_6^6 is much smaller than the axial anisotropy constants and can be ignored. In many calculations, the dipole-dipole interaction is also ignored, since it is only significant in a very small region at the center of the Brillouin zone. This is not valid for the long-wavelength regime relevant to light scattering; however, we will ignore the dipole-dipole and the Zeeman interactions at the moment and include them later. The resulting acoustic spin-wave dispersion is

$$\omega(\mathbf{q})=\frac{2S}{\hbar}\{[J(\mathbf{0})-J(\mathbf{q})][J(\mathbf{0})-J(\mathbf{q})+\sin^2\theta(P_2+6S^2P_4\cos^2\theta+15P_6S^4\cos^4\theta)]\}^{1/2}\ ,\tag{2}$$

obtained from Eq. (4.177) of Ref. 1. Here θ is the angle between the moments and the c axis, and $J(q)$ is the Fourier transformed exchange function; for small q it can be approximated by

$$J(\mathbf{0})-J(\mathbf{q})\approx\sum_i D_i q_i^2\ ,\tag{3}$$

where

$$D_i=2S\left|\frac{\partial^2 J}{\partial q_i^2}\right|_{\mathbf{q}=0}\ .$$

In the case of nearest-neighbor exchange in a cubic lattice with a coupling constant J, D is simply proportional to J. In Gd, D_i can be expressed as a sum of the interplanar exchange constants.

Now we introduce the dipole-dipole interaction that is significant in the long-wavelength limit. The geometry we are concerned with is that of a c-axis film with the moments and applied magnetic field lying in the plane of the film ($\theta=90°$) and the spin wave propagating perpendicular to the applied magnetic field. Using the above approximation for $J(q)$ and the geometry mentioned, the long-wavelength dispersion of a dipole-exchange bulk magnon in a thick file is given by

$$\omega(\mathbf{q})=\left[\left[\gamma H+\sum_i D_i q_i^2\right]\left[\gamma(H+H_a+4\pi M)+\sum_i D_i q_i^2\right]\right]^{1/2}\ ,\tag{4}$$

where $\gamma=g\mu_B/\hbar$ is the gyromagnetic ratio, and $H_a=2SP_2/(\sigma\hbar)$ is the effective anisotropy field where σ is the reduced magnetization $M(T)/M(0)$.

In a thin magnetic film, the spin waves can only propagate along the plane of the film. Standing wave solutions exist in the component normal to the surface. For such waves propagating perpendicular to the applied field, the energies are degenerate. However, the exchange interaction lifts this degeneracy. When surface anisotropy is either negligible or infinitely strong at both surfaces, the dispersion of these modes in the stated geometry is given by Eq. (4) if one replaces q_z with $\pi n/L$ where the z axis is normal to the film, L is the thickness of the film, and n is a non-negative integer. Therefore, for the case of interest where the c axis is along z, we obtain the following dispersion relation:

$$\begin{aligned}
&\omega(\mathbf{q}_\parallel)=\left\{\left[\gamma H+D_c\left[\frac{n\pi}{L}\right]^2\right]\left[\gamma(H+H_a+4\pi M)+D_c\left[\frac{n\pi}{L}\right]^2\right]\right\}^{1/2}+4\pi M H_a\left[\frac{q_\parallel^2}{q_\parallel^2+q_z^2}\right]\ ,\\
&\mathbf{q}_\parallel=(q_x,q_y)\ ,
\end{aligned}\tag{5}$$

where $D_a q_a^2$ and $D_b q_b^2$ are taken to be negligible. The $(q_z = \pi m/L)$ mode will be referred to as the $(n = m)$ bulk mode. In general, the dispersion relation for films with arbitrary surface anisotropy needs to be solved computationally. Equation (5) fits the data reasonably well and will be used in analyzing the observed spin-wave dispersion. However, an exact treatment would require the introduction of surface anisotropy in the spin-wave dispersion calculations.[12] Currently, the surface anisotropy constants of gadolinium are not known.

B. Surface spin waves

Surface spin waves propagate parallel to the surface with an amplitude decaying exponentially into the medium. In the magnetostatic limit, the surface spin wave exhibits nonreciprocal behavior and is also referred to as the Damon-Eshbach mode. The direction of propagation of this mode on the top surface of a film (defined to lie in the $+z$ direction from the film center) is restricted to an angular region about the positive x axis if the field is applied along the $+y$ direction. The complementary surface wave on the bottom surface propagates in the opposite direction. In a thick film the penetration depth is equal to $\lambda/2\pi$ where λ is the wavelength of the Damon-Eshbach mode. However, for films with thicknesses less than the surface wave penetration depth, this mode is no longer localized at the surfaces, and its frequency approaches the $n=0$ bulk mode frequency in the limit of zero thickness. In the absence of magnetic anisotropy, the frequency dispersion of the Damon-Eshbach mode is

$$\omega(\mathbf{q}_\parallel)=\gamma[(H+2\pi M)^2-4\pi^2M^2\exp(-2q_\parallel L)]^{1/2} \tag{6}$$

as given by Eq. (8.31) of Ref. 10. Including the effects of bulk anisotropy results in the implicit transcendental equation shown below:

$$\omega(\mathbf{q}_\parallel)^2=\frac{1}{2}\left[\omega_1^2+\gamma^2H\{H+H_a\}+\left[[\omega_1^2-\gamma^2H(H+H_a)]^2+\frac{4\eta}{\alpha}\gamma^4H(4\pi M)^2(H+H_a-r^2H)\right]^{1/2}\right], \tag{7}$$

where

$$\omega_1^2=\gamma^2[H(H+H_a+8\beta\pi M/\alpha)+(\eta/\alpha)(4\pi M)^2],$$

$$\alpha=(r+1)^2-(r-1)^2\exp(-2rq_\parallel L), \tag{8}$$

$$\beta=r(r+1)-r(r-1)\exp(-2rq_\parallel L),$$

$$\eta=1-\exp(-2rq_\parallel L),$$

and the dimensionless constant r is given by

$$r=\left[1-\frac{4\pi MH_a}{\omega^2-H(H+4\pi M+H_a)}\right]^{1/2}. \tag{9}$$

ω_1 reduces to the right-hand side of Eq. (6) when H_a is set to zero. Equation (7) was derived using the relations in Ref. 12. We solved it numerically.

IV. RESULTS AND DISCUSSION

A. Brillouin spectra

The depolarized Brillouin spectra for the 300-Å Gd film at $T=200$ K for applied magnetic field intensities of 1.0 and 4.8 kOe are shown in Figs. 4(a) and 4(b). The magnetic field was applied in the plane of the film and perpendicular to the scattering plane. The Damon-Eshbach mode can easily be identified in both spectra due to the large intensity asymmetry between the Stokes and anti-Stokes components, characteristic of these modes. Strictly speaking, these modes are not true surface waves, since the penetration depth of this wave is on the order of 1000 Å, while the film thickness is 300 Å. However, these modes transform into a surface wave in the limit of a very thick film. For identification purposes, these modes will be labeled as a shallow surface mode (SSM).

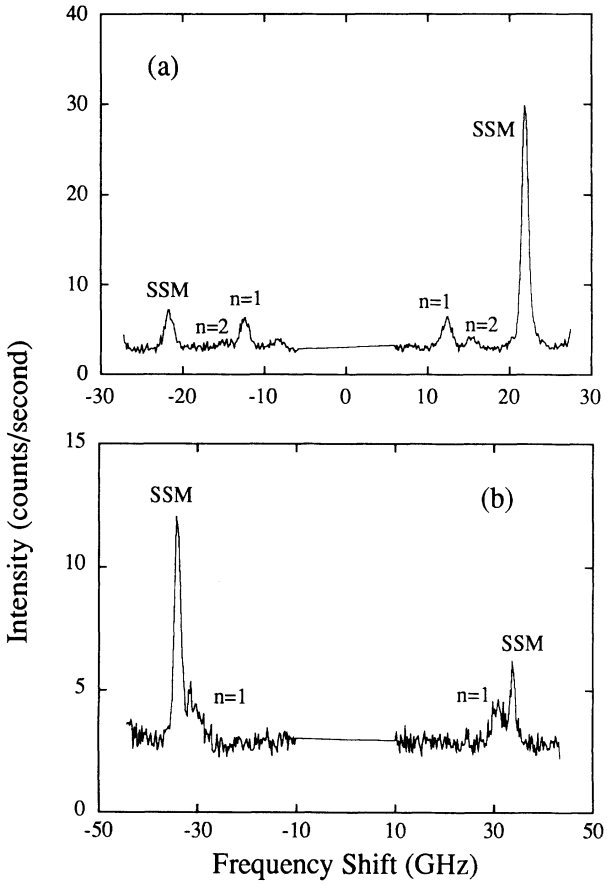

FIG. 4. The depolarized Brillouin spectra for the 300-Å Gd film. The "elastic" portion of the spectrum near $\omega=0$ has been excluded. (1) $T=200$ K, $H=1.0$ kOe, and $q=1.37\times10^5$ cm^{-1}. (b) $T=200$ K, $H=4.8$ kOe, and $q=9.41\times10^4$ cm^{-1}.

The remaining peaks are identified as the $n=1$ and 2 bulk modes as defined in Sec. III A. Note that the $n=2$ bulk mode is not resolvable in the $H=4.8$-kOe spectrum. The dispersion of the shallow surface and bulk modes was followed by varying the backscattering angle from a few degrees to about 60° [Figs. 5(a) and 5(b)]. Beyond 60°, the signal was very weak, as less light penetrated the metallic surface. The spectral peaks were fitted with Lorentzians. The magnetic-stiffness constant D_c was calculated from the frequency separation of the two bulk peaks observed in the $H=1.0$-kOe spectrum and is dependent on our assignment of these bulk modes. By considering different assignments, it was found that the $n=1$, $n=2$ assignment provides the best fit to the values calculated from Eq. (5) using the magnetization data taken on the 300-Å Gd film. The comparison was made with respect to the relative positions of the surface and bulk peaks rather than the absolute positions, which are influenced more by the uncertainties in the temperature, spectral calibration and film thickness. The overall offset in Fig. 5(a) between the Brillouin data and the dispersion curves calculated from the magnetization is due to these uncertainties. The offset in Fig. 5(b) is much larger and is partially due to the onset of axial anisotropy, which becomes significant below 200 K. The effect of axial anisotropy on the magnon frequency is not included in the calculation of the curves in Figs. 5(a) and 5(b). The data in Fig. 5(a) were taken at 200 K where axial anisotropy is negligible in bulk Gd (Fig. 8), and the data in Fig. 5(b) were taken at 100 K where axial anisotropy is significant.

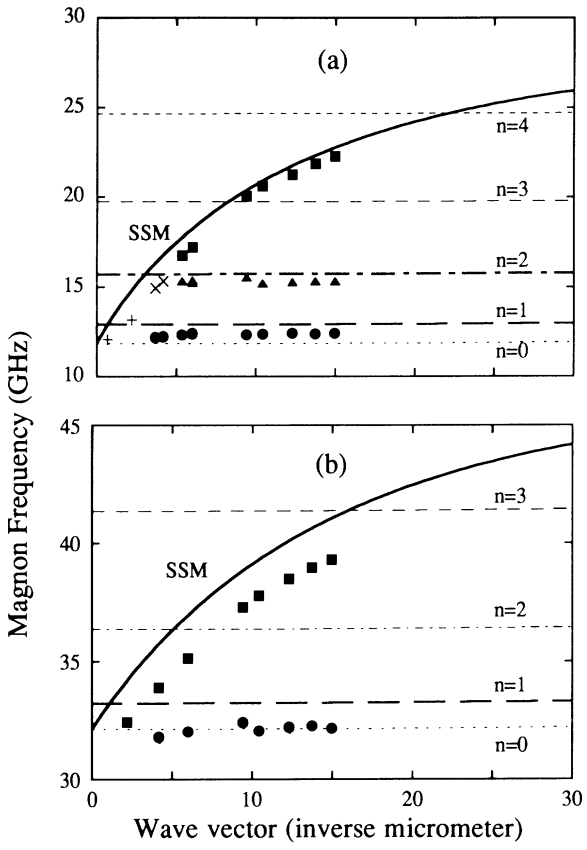

FIG. 5. The dispersion of the magnon frequencies extracted from the Brillouin data on the 300-Å Gd film compared with the curves calculated from Eq. (5) and Eq. (6) using the values for D_c determined from the Brillouin data and the values for the magnetization from the SQUID measurements. The effect of axial anisotropy is not included in the calculation. (a) $T=200$ K, $H=1.0$ kOe. (b) $T=100$ K, $H=4.8$ kOe. The Brillouin data are designated by the following markers: (■) shallow surface mode (SSM), (●) $n=1$ bulk mode, (▲) $n=2$ bulk mode, (+) $n=1+$SSM, and (×) $n=2+$SSM.

No selection rules exist that would prohibit the observation of the $n=2$ bulk mode, but it is possible for its spectral peak to be lost in the spectral peak of the $n=1$ bulk mode. Therefore, the alternate assignment of the peaks as the $n=1$ and 3 bulk modes is feasible, and in fact, it gives better agreement for the absolute positions of the bulk modes. However, this assignment gives poorer agreement in the relative positions of all the modes. Furthermore, the values for D extracted from the $n=1$, $n=2$ assignment compare more favorably with the values extracted from the neutron-scattering data. The $n=0$, $n=1$ assignment gives poor agreement both in the absolute and relative values. The $n=0$ bulk mode is normally not observed in Brillouin studies of ferromagnets.

The dispersion of the spin waves observed by light scattering compares well with the dispersion calculated from the dipole exchange dispersion relations. The dispersionless behavior of the bulk wave peaks also confirms our assignment of these peaks as due to light scattering from spin waves rather than elastic waves.

B. Temperature dependence

By analyzing the temperature dependence of the spectra, the temperature dependences of the c-axis magnetic-stiffness constant D_c and the magnetic axial anisotropy constant P_2 were extracted. A substantial portion of the temperature dependence of the spin-wave frequency was due to its strong dependence on the magnetization, and this was taken into account using the SQUID results from the Gd film.

1. C-axis magnetic surface constant

D_c was extracted from the frequency difference between the $n=1$ and 2 bulk modes. The effects of bulk anisotropy have been omitted, since it does not change the results significantly, and the effects of surface anisotropy have been omitted, since the relevant data is not available. Since the peaks from the $n=2$ bulk mode were weak and resolvable only in the temperature range from 180 to 250 K, (Fig. 6) the extracted temperature dependence of D_c is limited to this range. In order to make a rough extrapolation to temperatures below 180 K, the data for D_c were fitted with a power law in the magnetization of the 300-Å Gd film ($H=1.0$ kOe).

$$D_c=(7400\pm600)\sigma^{1.33\pm0.15}$$

resulted in the best fit where $\sigma=M(T)/M(0)$. The quoted uncertainties are from fitting and do not include the uncertainties in the data points. Setting $D\propto\sigma^p$ is strictly

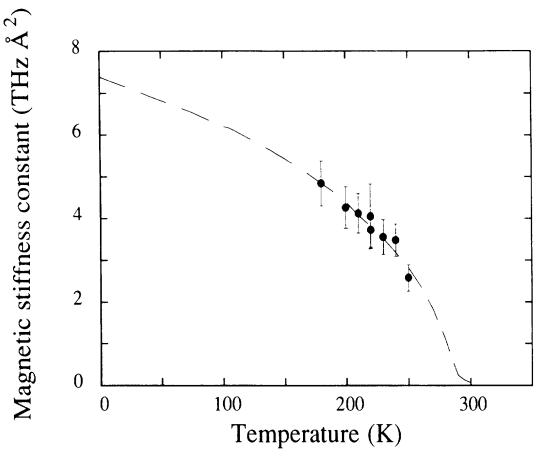

FIG. 6. The extracted values for the magnetic stiffness constant D_c of the 300-Å Gd film (circles) fit to $D_c = D_0\sigma^p$ (dashed line) where D_0 and p are the fitting parameters and σ is the reduced magnetization. An exponent of $p = 1.33 \pm 0.15$ and $D_0 = 7400 \pm 600$ GHz Å^2 resulted in the best fit.

valid only near the Curie temperature and when $H = 0$, but since D_c does not change very rapidly well below the Curie temperature, this should give a reasonable estimate for the value of D_c at low temperatures. However, the functional form would not be correct.

It is still worth while to compare the extracted exponents with the critical exponent expected for magnetic-stiffness constants even though rigorous conclusions cannot be drawn from the comparison. The $H = 1.0$-kOe magnetization curve was fitted with the power law $(T_c - T)^s$ in the temperature range 180–260 K (Fig. 7). The fit is very good in this region and gives a value of $s = 0.374 \pm 0.01$ and $T_c = 285 \pm 1.5$ K. Since $H \neq 0$ and T is not near T_c, it is not valid to call s the critical exponent β or to say the Curie temperature is 285 K.

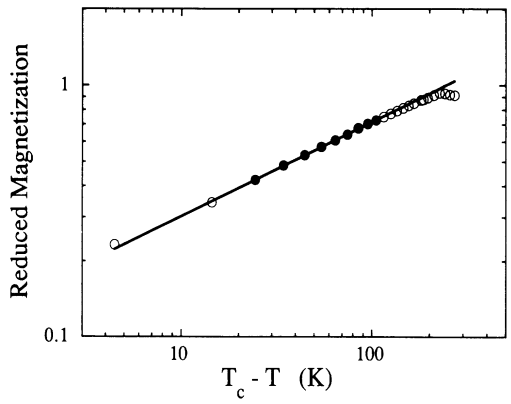

FIG. 7. The magnetization curve for the 300-Å Gd film ($H = 1.0$ kOe) shown in Fig. 1 plotted on a log-log plot in order to fit the magnetization to the power law $(T_c - T)^s$ in the temperature range, 180 K $< T <$ 260 K. $s = 0.374 \pm 0.1$ and $T_c = 285 \pm 1.5$ K resulted in the best fit, denoted by the straight line. The data points used in the fit are marked by filled circles. The remaining data points are marked by open circles.

Nevertheless, s is within the experimental uncertainties of β for bulk Gd, $\beta = 0.381 \pm 0.015$.[13] This power law for M implies that $D_c \propto (T_c - T)^{0.51 \pm 0.06}$ for 180 K $< T <$ 260 K. The magnetic-stiffness constant D is predicted to scale as

$$\xi^{-1}(T_c - T)^{-\beta} \propto (T_c - T)^{\nu' - \beta}$$

(Ref. 14). For Gd this implies

$$D_c \propto (T_c - T)^{0.272 \pm 0.005} \propto M^{0.714 \pm 0.010}$$

when using the following exponents: $\beta = 0.381 \pm 0.015$ and $\gamma = 1.196 \pm 0.003$ according to Ref. 13 and $\nu' = \nu = (2\beta + \gamma)/d = 0.653 \pm 0.01$ from scaling laws.

It is clear that the predicted power law disagrees with the power law observed in the 300-Å Gd film. A power law that would fit the magnetic-stiffness data with the predicted exponent would require the Curie temperature to be 262 K. This is well outside the experimental uncertainties of the Curie temperature of the 300-Å Gd film. However, it is not clear whether the discrepancy is a result of (1) neglect of the surface anisotropy in the model used to extract the magnetic stiffness, (2) an instrumental effect, or (3) a magnetic property of gadolinium whether in the bulk or in the film. More data and careful analysis are needed if this discrepancy is to be verified or resolved. The temperature readings should be carefully calibrated. A preliminary attempt at recalibration by assuming a constant 5-K shift in temperature due to laser heating results in only a slightly modified power law, $D_c \propto M^{1.2 \pm 0.2}$. Furthermore, the effects of surface anisotropy should be included. However, currently the main motivation for fitting the stiffness constants to a power law is to make an extrapolation to lower temperatures.

Note that the obtained values of D_c compare reasonably well with the values extract from inelastic neutron-scattering experiments on magnons in bulk Gd (Table I).[15] We estimated two values of D_c from the neutron data by fitting the first data point in the magnon dispersion and the point at the origin to a quadratic. The value of 5800 GHz Å^2 listed in this table was derived from the first five interplanar exchange constants listed in Ref. 15. These approximations made using the neutron data can give only a rough estimate for D_c, since the neutron data refer to wave vectors relatively far from the Brillouin-zone center; nevertheless, they are consistent with the values determined by Brillouin scattering. Since the data

TABLE I. The values for the magnetic-stiffness constant D_c extracted from the Brillouin data are compared with estimates of D_c made from the neutron data in Ref. 15. The value in parentheses is an extrapolation.

T	D_c (GHz Å^2) Brillouin	Neutron[a]
78 K	(6500)	6900, 5800
230 K	3600±400	3000

[a]Reference 15.

from neutron scattering do not cover a complete temperature range, the power-law behavior in the bulk cannot be compared with the behavior observed in the film.

2. *Axial anisotropy*

The extrapolation of D_c was used in the calculation of the temperature dependence of the bulk wave frequencies. In this calculation, the magnetic anisotropy of Gd must also be taken into account. If the comparison of the experimental data with the calculated curves were made while neglecting anisotropy, noticeable disagreement would be observed below 150 K [Fig. 5(b)]. Note, however, that the softening in the spin-wave frequency with decreasing temperature for the $H=4.8$-kOe experiment [Fig. 9(b)] is only partially due to the onset of anisotropy; the temperature dependence of the applied magnetic field accounts for part of this observed anomaly (see Fig. 3). The temperature dependence of the anisotropy constants for bulk Gd have been measured by torque magnetometer[16,17] and magnetization curve[18] methods; however, the data differs from group to group. Part of the variation is due to the magnetic-field dependence of the anisotropy constants. In all cases, P_2 is nearly zero at 200 K. Therefore, instead of using these results to correct for the calculated curves, the axial anisotropy constant P_2 was extracted from the Brillouin data for the shallow surface mode and compared with the values for bulk Gd (Fig. 8).

In extracting P_2, an offset was added to the calculated curve so that the Brillouin data coincide with it at 200 K, where P_2 was assumed to be zero. We chose P_2 in order to achieve agreement between the calculated and experimental curves below 200 K. These values for P_2 lie within the data spread seen in bulk Gd and have a similar functional form. The noticeable difference between the extracted values of P_2 for the two different applied magnetic-field strengths is not unexpected, as the field dependence of P_2 is significant between 0 and 5.0 kOe.[16,17]

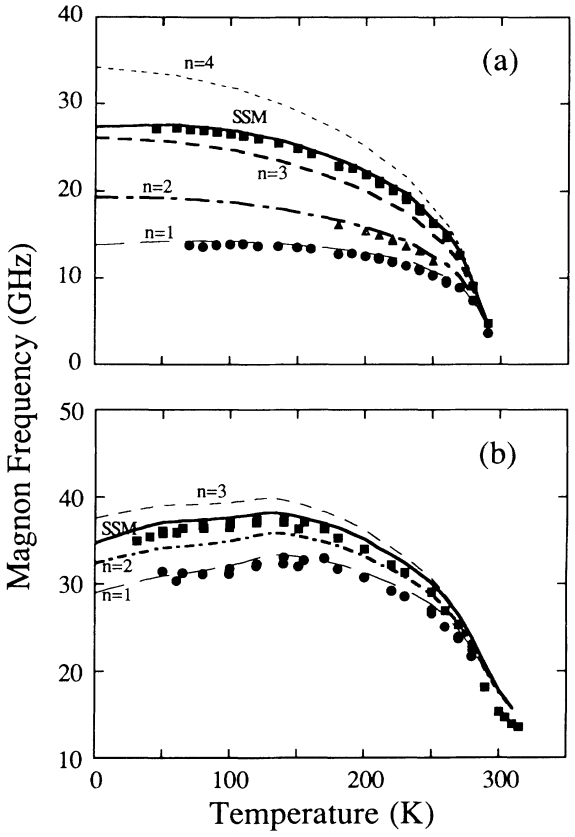

FIG. 9. The temperature dependences of the magnon frequencies extracted from the Brillouin data on the 300-Å Gd film compared with the curves calculated from Eq. (5) and Eq. (6) using the fit for $D_c(T)$ shown in Fig. 6, $P(T)$ from Fig. 8 and the respective magnetization curves from Fig. 1. (a) $H=1.0$ kOe, $q=1.37\times10^5$ cm^{-1}. (b) $H=4.8$ kOe, $q=9.41\times10^4$ cm^{-1}. The Brillouin data are designated by the following markers: (■) shallow surface mode, (●) $n=1$ bulk mode, and (▲) $n=2$ bulk mode.

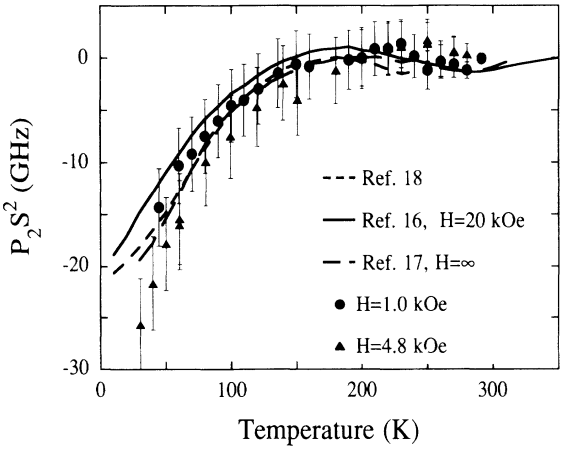

FIG. 8. The axial anisotropy constant P_2 for the 300-Å Gd film with $H=1.0$ kOe (squares) and $H=4.8$ kOe (triangles) compared with the bulk values from Fig. 160 in Ref. 1, which displays data extracted from Refs. 15–17. P_2S^2 is plotted vs temperature where $S=7/2$.

The extracted values for P_2 compare reasonable well with the bulk anisotropy data within the experimental uncertainties. This suggests that any additional anisotropy is not substantial in the 300-Å film. The comparison of the spin-wave dispersion calculated from the extracted values of P_2 and the magnetic-stiffness constants with the experimental data is displayed in Fig. 9, and the comparison is also good. Therefore, within the experimental uncertainties, the bulk anisotropy and the exchange and dipole-dipole interactions can reasonably account for the temperature dependence of the spin-wave frequencies in the 300-Å Gd film (Fig. 9).

V. CONCLUSIONS

A shallow magnetostatic surface wave and two bulk acoustic spin waves in a 300-Å Gd file have been

identified by use of Brillouin spectroscopy. The temperature dependence and the dispersion of the frequency of these spin waves were shown to fit a dipole-exchange model. From the fit to the data, we were able to extract the c-axis magnetic-stiffness constant D_c and the anisotropy constant P_2 over a limited temperature range.

The magnetic-stiffness constant D_c was extracted from the frequency difference between the $n=1$ and 2 bulk modes. The temperature dependence of D_c was fit to a $[M(T)]^{1.33\pm0.15}$ power law between 180 and 250 K, which was used to make a rough extrapolation of D_c to lower temperatures. The observed spin-wave dispersion complements, and is consistent with, the neutron data taken on bulk Gd, since reasonable estimates of D_c from the neutron data are comparable with the light-scattering values. However, the power-law fit of D_c does not compare well with that predicted by scaling theory. It must be remembered that surface anisotropy was ignored and the fit is for data at temperatures from $0.6T_c$ to $0.9T_c$ where predictions from scaling theory may not apply. Furthermore, the effect of local laser heating has not been included but is important in determining an accurate value of the exponent for D_c. A more detailed study might be initiated, but would be limited by the ability to resolve the $n=1$ and 2 bulk mode spectral peaks, which merge together near the Curie temperature.

The axial anisotropy constant P_2 was extracted from the measured temperature dependence of the shallow surface mode frequency. The extracted temperature dependence of P_2 is consistent with the values determined by torque magnetometer and magnetization curve methods; no substantial additional anisotropy was observed in the 300-Å film. Furthermore, the overall fit of the experimental data to the dispersion curves calculated from the extracted axial anisotropy and magnetic-stiffness constants is good. Therefore, within the experimental uncertainties, the temperature dependence of the spin-wave frequencies can be accounted for by the bulk magnetic properties of Gd.

ACKNOWLEDGMENTS

S. H. K. is grateful to Professor M. B. Salamon for sharing his insight on magnetism and making helpful comments on the paper and to Professor D. L. Mills and Mr. R. P. Erickson for discussion and correspondence concerning spin waves in ferromagnetic films. This research was supported by the National Science Foundation through Contract No. NSF-DMR 88-20888.

[1]B. Coqblin, *The Electronic Structure of Rare-Earth Metals and Alloys: the Magnetic Heavy Rare Earths* (Academic, London, 1977).

[2]R. W. Erwin, J. J. Rhyne, M. B. Salamon, J. A. Borchers, S. Sinha, R. Du, J. E. Cunningham, and C. P. Flynn, Phys. Rev. B **35**, 6808 (1987).

[3]C. F. Majkrzak, J. W. Cable, J. Kwo, M. Hong, D. B. McWhan, Y. Yafet, J. V. Waszczak, and C. Vettier, Phys. Rev. Lett. **56**, 2700 (1986).

[4]J. A. Borchers, M. B. Salamon, R. Du, C. P. Flynn, J. J. Rhyne, and R. W. Erwin, J. Appl. Phys. **63**, 3458 (1988).

[5]R. T. Demers, S. Kong, M. V. Klein, R. Du, and C. P. Flynn, Phys. Rev. B **38**, 11 523 (1988).

[6]P. Grünberg and F. Metawe, Phys. Rev. Lett. **39**, 1561 (1977).

[7]J. R. Sandercock and W. Wetling, IEEE Trans. Mag. **14**, 442 (1978).

[8]J. W. Cable and W. C. Koehler, J. Appl. Phys. **53**, 1904 (1982).

[9]J. Kwo, E. M. Gyorgy, D. B. McWhan, M. Hong, F. J. Di Salvo, C. Vettier, and J. E. Bower, Phys. Rev. Lett. **55**, 1402 (1985).

[10]M. G. Cottam and D. J. Lockwood, *Light Scattering in Magnetic Solids* (Wiley, New York, 1986).

[11]R. E. Camley, Talat S. Rahman, and D. L. Mills, Phys. Rev. B **23**, 1226 (1981).

[12]G. T. Rado and R. J. Hicken, J. Appl. Phys. **63**, 3885 (1988).

[13]M. N. Deschizeaux and G. Devely, J. Phys. (Paris) **32**, 319 (1971).

[14]B. I. Halperin and D. C. Hohenberg, Phys. Rev. **177**, 952 (1969).

[15]W. C. Koehler, H. R. Child, R. M. Nicklow, H. G. Smith, R. M. Moon, and J. W. Cable, Phys. Rev. Lett. **24**, 16 (1970).

[16]C. D. Graham, Jr., J. Appl. Phys. **34**, 1341 (1963).

[17]W. D. Corner, W. C. Roe, and K. N. R. Taylor, Proc. Phys. Soc., London. **80**, 927 (1962); B. Coqblin and W. D. Corner (private communication).

[18]J. L. Feron, Ph.D. thesis, University of Grenoble, 1969.